ACS OMEGA

http://pubs.acs.org/journal/acsodf

Article

How the Environment Encourages the Natural Formation of Hydrated V_2O_5

Rahul Parmar,* Matteo Amati, Luca Gregoratti,* Seyed Javad Rezvani, Pritam Banerjee, Piu Rajak, Regina Ciancio, and Roberto Gunnella

Cite This: *ACS Omega* 2022, 7, 31115−31119

Read Online

ACCESS | Metrics & More | Article Recommendations

ABSTRACT: Herein, we report the microscopic and spectroscopic signatures of the hydrated V_2O_5 phase, prepared from the α-V_2O_5 powder, which was kept in deionized water inside an airtight glass container for approximately 2.5 years. The experimental results show an evolution of the V^{4+} component in V $2p_{3/2}$ core energy level spectra, and a peak corresponding to σ-OH^- bond appeared in the valence band spectra in the hydrated V_2O_5 powder sample due to the water intercalation. Vanadium metal oxide particles were found to be self-nucleated into micro/nanorods after a long period of exposure to an extremely humid environment. The distinct features in the spectra obtained with high-resolution transmission electron microscopy, micro-Raman scattering, and X-ray photoelectron spectroscopy confirmed the presence of structural water molecules for the first time in the long-aged naturally hydrated V_2O_5 phase.

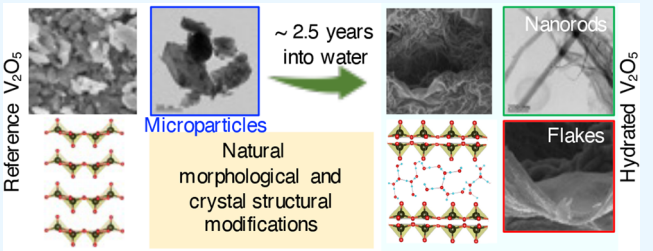

INTRODUCTION

The structural instability of the orthorhombic α-V_2O_5 (space group *Pmmn*) phase has emerged as a constraint for the multication battery design. The interplanar distance of 4.36 Å between $[VO_5{-}VO_5]$ polyhedra chains in α-V_2O_5 may not be able to host reversibly large ionic radius cations into its crystal volume for a long-lifetime. For this reason, it may undergo irreversible structural deformation after a certain number of charge/discharge cycles. V_2O_5 has a wide range of applications in electrochromic, photochromic devices, gas sensors (ammonia, ethanol, pH sensor, NO_2, H_2O_2, etc.), biosensors (urea, glucose, gene sequence, methylglyoxal etc.) smart glass windows in satellites, and aerospace vehicles.[1−4] The device performance may be reduced due to the degradation or permanent modifications in the V_2O_5 material in contact with humidity for a long-lifetime. However, the hydrated V_2O_5, which has water gradients in its structures, can be a suitable material for the long life application where a humid environment is the working condition. The hydrated V_2O_5 can be synthesized by the several methods such as sol−gel, hydrothermal, electrochemical, xerogel, etc.[5−11] In the past, numerous experimental and theoretical studies have been reported on the impact of water molecules into the V_2O_5 local structure, its electronic, electrical properties, multications insertion/extraction mechanisms, charge transfer, and energy band gap tuning.[12−15] Water insertion into the V_2O_5 structure breaks the symmetry and inverts the $[VO_5^-]$ polyhedra along the *c*-axis direction resulting in an increase of the interplanar distance up to ~15 Å.[16] The presence of structural water (free protons, i.e., H^+ ions) may improve the electronic or ionic conductivity.[17] Thus, spectroscopic investigation of the chemisorbed and intercalated water gradient into the V_2O_5 local structure becomes imperative to study the reference signatures. We demonstrate here, how the V_2O_5 modifies its structure after having been kept in water for more than two years (~2.5 years) at ambient conditions. The reported experimental evidence in this article is based on chemical reactions occurring at natural environmental conditions typical for the long lifetime application of the reported material.

RESULTS AND DISCUSSION

Scanning electron microscopy (SEM) images of reference and hydrated V_2O_5 powder (see Figure 1a) show the significant surface morphology modifications, where the micron and submicron sized reference V_2O_5 powder particles (Figure 1b) merged to form wrinkled, porous, and self-nucleated nano/microrod mesh-like structures in the hydrated V_2O_5 sample (Figure 1e). The dimensions (length/width) of the microparticles of the reference V_2O_5 powder sample was calculated

Received: May 24, 2022
Accepted: July 28, 2022
Published: August 22, 2022

Downloaded via UNIV DI CAMERINO on December 7, 2023 at 08:29:52 (UTC).
See https://pubs.acs.org/sharingguidelines for options on how to legitimately share published articles.

ACS Publications

© 2022 The Authors. Published by American Chemical Society

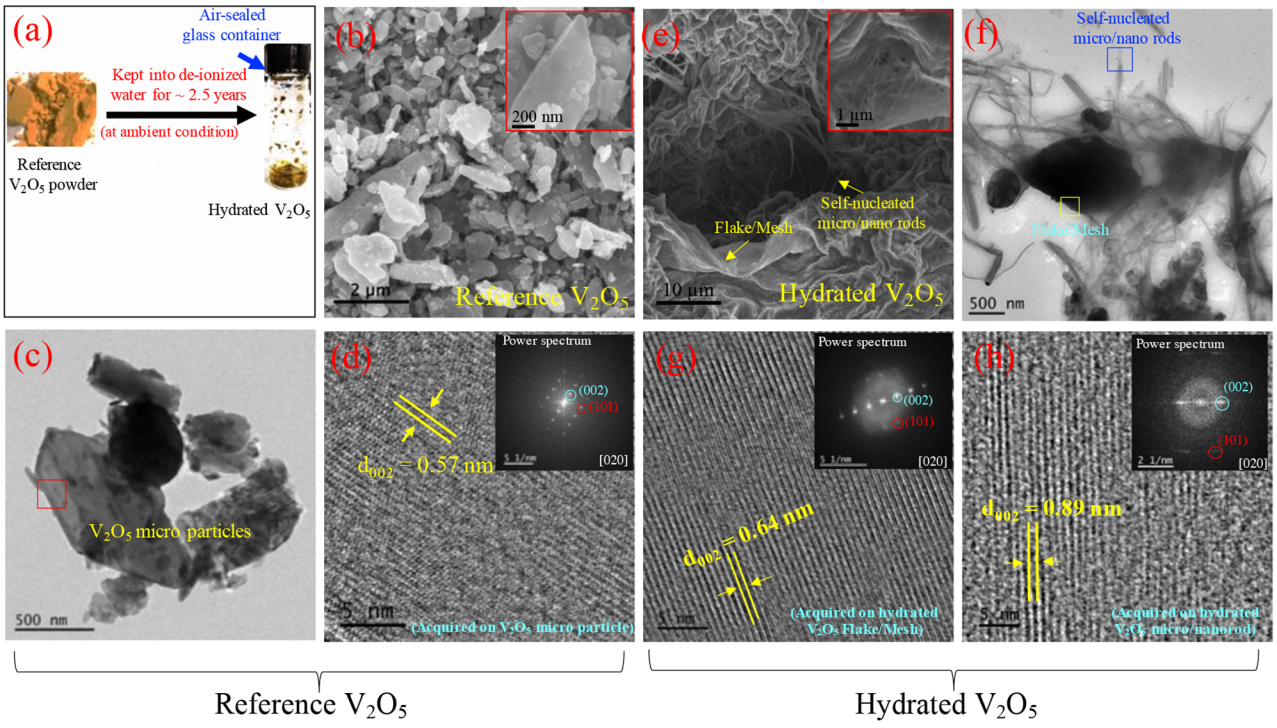

Figure 1. Reference V_2O_5 (Sigma-Aldrich) and hydrated V_2O_5 powder (kept into deionized water after ~2.5 years) samples images (a), scanning electron microscopy (SEM) images (b,e), bright field and high-resolution transmission electron microscopy (HRTEM) images (f,c), and filtered lattice images of the reference V_2O_5 (d) and hydrated V_2O_5 (g,h) samples, respectively. The power spectrum generated from the lattice images is shown in the insets. HRTEM lattice images were acquired on the selected area (drawn by solid line squares) as shown in respective bright field images of the reference and hydrated V_2O_5 samples. The magnified SEM images of reference and hydrated V_2O_5 samples are shown in inset images of Figure 1b,e, respectively.

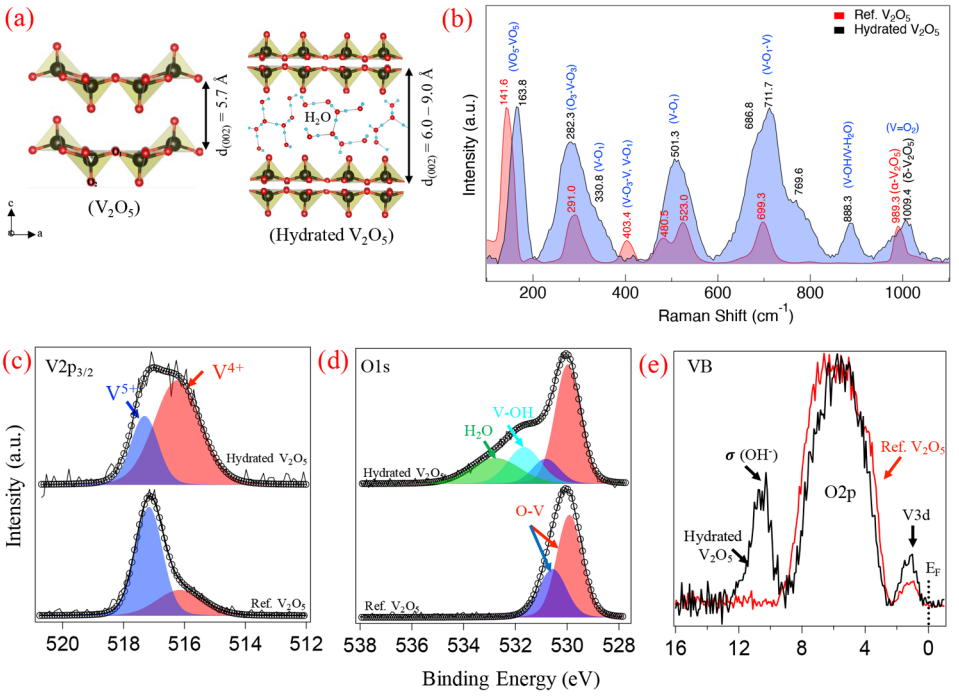

Figure 2. Electronic structures of reference and hydrated V_2O_5 phase (a), micro-Raman scattering spectra (b), and X-ray photoelectron spectroscopy (XPS) core energy level spectra of the reference and hydrated V_2O_5 powder samples, V $2p_{3/2}$ (c), O 1s (d), and VB (e), respectively.

in the range from 0.2 to 2.0 μm, while the nanorods in the hydrated V_2O_5 sample have a diameter ranging from ~30 to 130 nm. The flakes/meshes-like morphological features in the hydrated V_2O_5 sample (Figure 1e) have a thickness ranging from ~30 to 50 nm. The bright field HRTEM images of reference (Figure 1c) and hydrated (Figure 1f) V_2O_5 samples

https://doi.org/10.1021/acsomega.2c03236
ACS Omega 2022, 7, 31115−31119

support the findings of the SEM results. From the lattice images (Figure 1d,g,h), the measured interplanar spacing corresponding to the (002) plane, was calculated to be ∼0.57 and 0.64, 0.89 nm for the reference and hydrated V_2O_5 phases, respectively. The flakes/meshes showed less *d*-spacing values than the nanorod-like structures in the hydrated V_2O_5 sample. This implies that the flakes/meshes formation was an intermediate stage of hydration process before the micro/nanorods formation, which had a high gradient of water inside the structure. A substantial increase of interplanar spacing along the *c*-axis is evidence of water molecules intercalating between the layered V_2O_5 structure, resulting in an expansion of the crystal volume. Thus, both SEM and HRTEM results corroborate that a long exposure of α-V_2O_5 to deionized water modifies its structure into the hydrated V_2O_5 (δ-V_2O_5).

Figure 2a illustrates the basic electronic structures of α-V_2O_5 and hydrated V_2O_5. The Raman spectrum of the hydrated V_2O_5 exhibits an enhancement of the peak intensity corresponding to the bridging O_1−V−O_3/V−O_1−V vibrational bonds (ranging from 200 to 700 cm^{-1}) and two additional Raman bands appearing at ∼769 and 888 cm^{-1} (V−OH vibrational bond) Raman shifts as compared to the reference V_2O_5 sample (see Figure 2b).[18,19] Consequently, the Raman shift of vanadyl bonds (V═O_2) was found blue-shifted along with the peak broadening in the hydrated V_2O_5 sample spectra, which may be due to the electrostatic interaction of water molecules or OH^- ions along the *c*-axis. These electrostatic forces may reduce the V═O_2 bond length, as a consequence of the volume expansion of the hydrated V_2O_5 unit cell, compared to the reference V_2O_5. The appearance of the additional Raman shifts, peak broadening, enhancement in peak intensity, and blue shift, indicates evidence of the presence of structural water into the hydrated V_2O_5 sample.[8] The HRTEM and Raman scattering results provide evidence of water molecule intercalation inside the V_2O_5 crystal structure at ambient conditions (the natural formation of hydrated V_2O_5). Furthermore, X-ray photoelectron spectroscopy (XPS) a surface sensitive technique was employed to verify the intercalated water into V_2O_5 (first layer of intercalated water molecules) by an escape depth of the electrons at a kinetic energy of oxygen (O 1s) and valence band core energy levels.

Figure 2 panels c and d show the O 1s, V $2p_{3/2}$, and VB core energy level XPS spectra of the reference and hydrated V_2O_5 powder samples. In the V $2p_{3/2}$ spectra (Figure 2c), the components at binding energies (BEs) of ∼516.3 ± 0.1 eV (fwhm = 1.8 eV) and 517.3 ± 0.1 eV (fwhm = 1.0 eV) are associated with V^{4+} and V^{5+} oxidation states, respectively.[20] The V^{4+} component contribution was increased in the hydrated V_2O_5 spectra compared to the reference V_2O_5 powder sample spectra, which may be due to the water molecules interaction with the [VO_5−VO_5] atomic layers and resulting in the reduction of V^{5+} to the V^{4+} oxidation state.[17] However, a residual presence of V^{4+} on the surface of reference V_2O_5 powder sample (Figure 2c) was due to the possible V_6O_{13} secondary phase.[21,22] In general, the reduction of vanadium (V^{5+}) in the V_2O_5 system occurs due to the loss of loosely bound lattice oxygen atoms. Furthermore, in O 1s core level spectra (Figure 2d), the BEs at value of ∼529.9 ± 0.1 eV (fwhm = 1.2 eV), 530.6 ± 0.1 eV (fwhm = 1.2 eV), 531.7 ± 0.1 eV (fwhm = 1.5 eV), and 532.8 ± 0.1 eV (fwhm = 2.3 eV) are assigned to vanadium−oxygen (V−O), V−OH, and H_2O chemical bonds in the reference and hydrated V_2O_5 samples, respectively.[23] The H_2O-related O 1s component is totally absent in the reference sample while it is clearly present in the hydrated one, providing a direct proof of the water presence. Due the dielectric property of the V_2O_5 (energy band gap = ∼2.3 eV), the VB spectra are dominated by the O 2p contribution,[24] associated with the three types of lattice oxygen bonds with vanadium, that is, V−O, O−V−O/V−O−V, and V═O in the V_2O_5 structure. The V 3d conduction band appeared at the BE of ∼1.1 eV below the Fermi energy (EF) level, due to the O 2p−V $3d_{xy}$ hybridization (Figure 2e). The V 3d component appeared because of the presence of the V^{4+} state, resulting in an increase of the electron density in the conduction band.[25−27] Most notably, the VB spectra of the hydrated V_2O_5 sample depicted the enhanced intensity (increased by the factor ∼2.0) of V 3d band along with an additional peak at the BE of ∼10.6 ± 0.3 eV assigned to the σ-(OH^-) chemisorbed bonds.[20] The O 2p line shape was slightly affected (become narrower) by the water molecules interaction in the hydrated V_2O_5 sample spectra.

In a complementary manner, the microscopic and spectroscopic data analysis depicted the natural phenomenon of H_2O molecules intercalation into the V_2O_5 local structure occurred by the kept into the deionized water for a long time period without any applied external electrical potential or other electrochemical forces. The mixed oxidation of V^{5+} and V^{4+} are associated with the $V_2O_5{\cdot}xVO_2{\cdot}nH_2O$ phase in case of the hydrated V_2O_5 phase.[28] The free electron density in the V 3d state of the hydrated V_2O_5 or reduced V_2O_5, contributed from $VO_{2\pm x}$ phase. The structural water increased the interplanar distance between the [VO_5−VO_5] polyhedra, calculated from HRTEM data, resulting in an increase of overall crystal volume of the hydrated V_2O_5 phase as proved by HRTEM diffraction analysis. The phase modification from α-V_2O_5 (∼990 cm^{-1}) to δ-V_2O_5 (∼1010 cm^{-1}) occurring due to an electrostatic interaction force from water molecules was observed.

CONCLUSION

The spectroscopic and microscopic signatures confirmed the hydrated V_2O_5 phase. These results may be considered as the reference signatures of the naturally aged hydrated V_2O_5 material. The reported results are important to distinguish the naturally hydrated V_2O_5 and hydration by the artificial methods in future related studies. The zero cost and natural method to produce the hydrated V_2O_5 nano/microrods, flake-like structure may replace the synthetic experimental ways. The self-nucleation of vanadium metal oxides micro/nanorods, like biological things growing in nature, is a new concept of material growth for the material science community.

EXPERIMENTAL SECTION

SEM images were captured by a ZEISS Gemini FE-SEM Sigma 300 instrument with a field emission gun at the Physics division, University of Camerino, Italy. Micro-Raman scattering spectroscopy (μ-RS) spectra were acquired by the HORIBA IHR320 apparatus equipped with a 50× objective lens (probing depth 500−800 nm) micro-Raman spectroscopy with an argon-ion green laser light source (λ = 532 nm) and grating system at 600 lines/mm at the Physics division University of Camerino, Italy. A constant value of the laser power (∼5 mW) was applied to avoid the internal thermal effect on both the reference V_2O_5 powder and the hydrated V_2O_5 sample. High resolution transmission electron microscopy (HRTEM) images and the selective area electron

https://doi.org/10.1021/acsomega.2c03236
ACS Omega 2022, 7, 31115−31119

diffraction (SAED) pattern were using a JEOL 2010 UHR field emission gun microscope operated at 200 kV with a measured spherical aberration coefficient (C_s) value of 0.47 ± 0.01 at the TASC laboratory, CNR-IOM, science park, Trieste, Italy. The TEM sample preparation of the reference and hydrated powder samples was followed by ultrasonication for 30 min in ethanol and deionized water, respectively. Later on, the powder samples were drop cast on the carbon coated Cu grid with 200 μm^2 mesh size. Scanning photoelectron microscopy (SPEM) at the ESCA microscopy beamline at the Elettra Synchrotron Light Center, Trieste, Italy, was employed to study the electronic structure modification before and after water intercalation into the V_2O_5 structure by analyzing the core energy level and valence band spectra. For the SPEM experiments performed in an ultrahigh vacuum (UHV) ($\sim 10^{-10}$ mbar) chamber, the powder samples were sandwiched between TEM grids, which were mechanically mounted between stainless steel clips to avoid any contamination and substrate effect. An incident photon energy of 650.0 eV (calibrated by Au 4f) was used to acquire the V 2p, O 1s, and valence band (VB) spectra. The hydrated V_2O_5 powder sample was subjected to heat treatment at 80 °C temperature inside the UHV chamber for 12 h, to remove the surface contamination and adsorbed water contents from the powder surface.

AUTHOR INFORMATION

Corresponding Authors

Rahul Parmar − *Elettra Sincrotrone Trieste SCpA, 34149 Basovizza, Trieste, Italy*; orcid.org/0000-0002-3439-7822; Email: rahul.parmar@elettra.eu

Luca Gregoratti − *Elettra Sincrotrone Trieste SCpA, 34149 Basovizza, Trieste, Italy*; Email: luca.gregoratti@elettra.eu

Authors

Matteo Amati − *Elettra Sincrotrone Trieste SCpA, 34149 Basovizza, Trieste, Italy*

Seyed Javad Rezvani − *Physics Division, School of Science and Technology, University of Camerino, 62032 Camerino, Macerata, Italy*; orcid.org/0000-0002-6771-170X

Pritam Banerjee − *CNR-IOM, TASC Laboratory in Area Science Park, 34139 Trieste, Italy*

Piu Rajak − *CNR-IOM, TASC Laboratory in Area Science Park, 34139 Trieste, Italy*

Regina Ciancio − *CNR-IOM, TASC Laboratory in Area Science Park, 34139 Trieste, Italy*; orcid.org/0000-0003-1739-3763

Roberto Gunnella − *Physics Division, School of Science and Technology, University of Camerino, 62032 Camerino, Macerata, Italy*; orcid.org/0000-0003-4739-6375

Complete contact information is available at: https://pubs.acs.org/10.1021/acsomega.2c03236

Notes

The authors declare no competing financial interest.

ACKNOWLEDGMENTS

Rahul Parmar thanks Elettra Synchrotron Trieste for a postdoctoral fellowship. Sara Mattiello, from Physics Division, University of Camerino, is acknowledged for the Raman scattering experiment. Co-authors P.B. and P.R. acknowledge receipt of a fellowship from the ICTP Programme for Training and Research in Italian Laboratories, Trieste, Italy.

REFERENCES

(1) Miyazaki, H.; Matsuura, T.; Ota, T. Vanadium oxide-based photochromic composite film. *RSC Adv.* **2017**, *7*, 2388−2391.

(2) Ma, C.; Taya, M.; Xu, C. Smart sunglasses based on electrochromic polymers. *Polym. Eng. Sci.* **2008**, *48*, 2224−2228.

(3) Cestarolli, D. T.; Guerra, E. M. In *TransitionMetal Compounds*; Haider, S., Haider, A., Eds.; IntechOpen: Rijeka, 2021; Chapter 2.

(4) Lin, T.-C.; Jheng, B.-J.; Huang, W.-C. Electrochromic Properties of the Vanadium Pentoxide Doped with Nickel as an Ionic Storage Layer. *Energies* **2021**, *14* (8), 2065.

(5) Du, G.; Seng, K. H.; Guo, Z.; Liu, J.; Li, W.; Jia, D.; Cook, C.; Liu, Z.; Liu, H. Graphene-V_2O_5·H_2O xerogel composite cathodes for lithium ion batteries. *RSC Adv.* **2011**, *1*, 690−697.

(6) Charles, D. S.; Feygenson, M.; Page, K.; Neuefeind, J.; Xu, W.; Teng, X. Structural water engaged disordered vanadium oxide nanosheets for high capacity aqueous potassium-ion storage. *Nat. Commun.* **2017**, *8*, 1−8.

(7) Li, Y.; Xu, P.; Jiang, J.; Yao, J.; Huang, B.; Yang, J. Facile synthesis of ultra-large V_2O_5 xerogel flakes and its application as a cathode material for aqueous Zn-ion batteries. *Materials Today Communications* **2021**, *26*, 101849.

(8) Parmar, R.; de Freitas Neto, D.; Matsubara, E.; Gunnella, R.; Rosolen, J. Electrochemical synthesis and structural characterization of nanostructured V_2O_5.nH_2O on CNTs coated/uncoated carbon felt composite. *Nano-Structures & Nano-Objects* **2020**, *24*, 100538.

(9) Parmar, R.; de Freitas Neto, D. B.; Matsubara, E. Y.; Gunnella, R.; Rosolen, J. M. Electro-insertion of Mn^{2+} ions into V_2O_5·H_2O on MWCNTs coated carbon felt for binder-free Na+ ion battery electrodes. *Sustainable Energy Fuels* **2020**, *4*, 3951−3962.

(10) De Freitas Neto, D.; Parmar, R.; Matsubara, E.; Minicucci, M.; Gunnella, R.; Rosolen, J. Nanostructured V_2O_5.nH_2O/cup-stacked carbon nanotube composite with remarkable Li+ specific capacity. *Solid State Ionics* **2021**, *363*, 115590.

(11) Bi, S.; Wang, S.; Yue, F.; Tie, Z.; Niu, Z. A rechargeable aqueous manganese-ion battery based on intercalation chemistry. *Nat. Commun.* **2021**, *12*, 1−11.

(12) Porsev, V. V.; Bandura, A. V.; Evarestov, R. A. Water adsorption on α -V_2O_5 surface and absorption in V_2O_5.nH_2O xerogel: DFT study of electronic structure. *Surf. Sci.* **2017**, *666*, 76−83.

(13) Kristoffersen, H. H.; Metiu, H. Structure of V_2O_5·H_2O Xerogels. *J. Phys. Chem. C* **2016**, *120*, 3986−3992.

(14) Petkov, V.; Trikalitis, P. N.; Bozin, E. S.; Billinge, S. J. L.; Vogt, T.; Kanatzidis, M. G. Structure of V_2O_5.nH_2O Xerogel Solved by the Atomic Pair Distribution Function Technique. *J. Am. Chem. Soc.* **2002**, *124*, 10157−10162.

(15) Simon, P.; Gogotsi, Y. Confined water controls capacitance. *Nat. Mater.* **2021**, *20*, 1597−1598.

(16) Moretti, A.; Passerini, S. Bilayered nanostructured V_2O_5.nH_2O for metal batteries. *Adv. Energy Mater.* **2016**, *6*, 1600868.

(17) Uchida, N.; Kittaka, S. Interlayer Water Molecules in Vanadium Pentoxide Hydrate, V_2O_5.nH_2O. 5. Dynamic Motion Analyzed by Impedance Measurements. *J. Phys. Chem.* **1994**, *98*, 2129−2133.

(18) Brown, E.; Acharya, J.; Elangovan, A.; Pandey, G. P.; Wu, J.; Li, J. Disordered Bilayered V_2O_5.nH_2O Shells Deposited on Vertically Aligned Carbon Nanofiber Arrays as Stable High-Capacity Sodium Ion Battery Cathodes. *Energy Technology* **2018**, *6*, 2438−2449.

(19) Glynn, C.; Creedon, D.; Geaney, H.; Armstrong, E.; Collins, T.; Morris, M. A.; Dwyer, C. O. Linking precursor alterations to nanoscale structure and optical transparency in polymer assisted fast-rate dip-coating of vanadium oxide thin films. *Sci. Rep.* **2015**, *5*, 1−15.

(20) Surnev, S.; Ramsey, M.; Netzer, F. Vanadium oxide surface studies. *Prog. Surf. Sci.* **2003**, *73*, 117−165.

(21) Chenakin, S. P.; Prada Silvy, R.; Kruse, N. Effect of X-rays on the Surface Chemical State of Al_2O_3, V_2O_5, and Aluminovanadate Oxide. *J. Phys. Chem. B* **2005**, *109*, 14611−14618.

(22) Mendialdua, J.; Casanova, R.; Barbaux, Y. XPS studies of V_2O_5, V_6O_{13}, VO_2 and V_2O_3. *J. Electron Spectrosc. Relat. Phenom.* **1995**, *71*, 249−261.

(23) Silversmit, G.; Depla, D.; Poelman, H.; Marin, G. B.; de Gryse, R. Determination of the V2p XPS binding energies for different vanadium oxidation states (V^{5+} to V^{0+}). *J. Electron Spectrosc. Relat. Phenom.* **2004**, *135*, 167−175.
(24) de Jesus, L. R.; Horrocks, G. A.; Liang, Y.; Parija, A.; Jaye, C.; Wangoh, L.; Wang, J.; Fischer, D. A.; Piper, L. F.; Prendergast, D.; et al. Mapping polaronic states and lithiation gradients in individual V_2O_5 nanowires. *Nat. Commun.* **2016**, *7*, 1−9.
(25) D'Elia, A.; Grazioli, C.; Cossaro, A.; Li, B.; Zou, C.; Rezvani, S.; Pinto, N.; Marcelli, A.; Coreno, M. Strain mediated Filling Control nature of the Metal-Insulator Transition of VO_2 and electron correlation effects in nanostructured films. *Appl. Surf. Sci.* **2021**, *540*, 148341.
(26) D'Elia, A.; Rezvani, S.; Zema, N.; Zuccaro, F.; Fanetti, M.; Belec, B.; Li, B.; Zou, C.; Spezzani, C.; Sacchi, M.; et al. Stoichiometry and disorder influence over electronic structure in nanostructured VO_x films. *J. Nanopart. Res.* **2021**, *23*, 1−9.
(27) D'Elia, A.; Rezvani, S.; Cossaro, A.; Stredansky, M.; Grazioli, C.; Li, B.; Zou, C.; Coreno, M.; Marcelli, A. Strain induced orbital dynamics across the metal insulator transition in thin VO_2/TiO_2 (001) films. *Journal of Superconductivity and Novel Magnetism* **2020**, *33*, 2383−2388.
(28) Lv, T. T.; Liu, Y. Y.; Wang, H.; Yang, S. Y.; Liu, C. S.; Pang, H. Crystal water enlarging the interlayer spacing of ultrathin $V_2O_5{\cdot}4VO_2{\cdot}2.72H_2O$ nanobelts for high-performance aqueous zinc-ion battery. *Chemical Engineering Journal* **2021**, *411*, 128533.

Recommended by ACS

Tracing Local Disorder in Near-Infrared-Upconverting Crystals of Li^+-Doped Gd_2O_3 through the Gd(III)-O Bond Distance

Preeti Verma, Supratim Giri, *et al.*
NOVEMBER 15, 2022
THE JOURNAL OF PHYSICAL CHEMISTRY C
READ

Suppression of Strain Relaxation in VO_2/TiO_2 Multilayered Films

Binjie Chen, Hiromichi Ohta, *et al.*
APRIL 04, 2023
ACS APPLIED ELECTRONIC MATERIALS
READ

Features of Phase Formation of Pyrochlore-type Ceramics $Bi_2Mg(Zn)_{1-x}Ni_xTa_2O_9$

Nadezhda A. Zhuk, Maria V. Yermolina, *et al.*
MARCH 16, 2023
ACS OMEGA
READ

Facile Synthesis of Pure and Cr-Doped WO_3 Thin Films for the Detection of Xylene at Room Temperature

Srinivasa Rao Sriram, Damodar Reddy Edla, *et al.*
DECEMBER 14, 2022
ACS OMEGA
READ

Get More Suggestions >

https://doi.org/10.1021/acsomega.2c03236
ACS Omega 2022, 7, 31115−31119